JOURNAL OF MATERIALS SCIENCE **38** (2003) 621 – 628

Crystal structure of $(Ba_{1-x}La_x)$ $[Mg_{(1+x)/3}Nb_{(2-x)/3}]O_3$ ceramics

JONG HOO PAIK, SAHN NAHM*
Department of Materials Science and Engineering, Korea University, Seoul 136-701, Korea
YOUNG SIK KIM
Department of Radio Science and Engineering, Korea University, Seoul 136-701, Korea
HYUN MIN PARK, HWACK JOO LEE
New Materials Evaluation Center, Korea Research Institute of Standards and Science, Taejon 305-600, Korea
JAE DONG BYUN
Department of Materials Science and Engineering, Korea University, Seoul 136-701, Korea

The crystal structure of $(Ba_{1-x}La_x)[Mg_{(1+x)/3}Nb_{(2-x)/3}]O_3$ (BLMN) ceramics with $0 \leq x \leq 1$ was investigated using X-ray diffraction (XRD) and high resolution transmission electron microscopy (HRTEM). When the La content, x, was above 0.1, the 1:2 ordered hexagonal structure found in $Ba(Mg_{1/3}Nb_{2/3})O_3$ (BMN) was transformed into the 1:1 ordered cubic structure. The 1:1 ordered cubic structure was maintained up to $x = 0.7$. When x exceeded 0.7, however, BLMN exhibited a 1:1 ordered monoclinic structure, rather than a 1:1 ordered cubic structure. $La(Mg_{2/3}Nb_{1/3})O_3$ (LMN) has a 1:1 ordered monoclinic $P2_1/n$ structure with $a = 5.6004$ Å, $b = 5.6414$ Å, $c = 7.9346$ Å, and $\beta = 89.9819°$. The monoclinic LMN has the in-phase and the anti-phase tilt of oxygen octahedra. The anti-parallel shift of A-site cations was also found in LMN. © *2003 Kluwer Academic Publishers*

1. Introduction

Complex perovskite ceramics have been extensively investigated for the application to the dielectric resonators at microwave frequencies [1]. The dielectric properties of these materials are largely affected by the structural properties. In particular, the chemical ordering of B site cations and the tilting of the oxygen octahedra are the major factors which influence Q vaule and the temperature coefficient of resonance frequency (τ_f) of these ceramics. According to the previous investigations, the 1:2 chemical ordering improved the Q value of the complex perovskite ceramics [2]. Tilting of the oxygen octahedra in simple perovskite was investigated by Glazer [3, 4] and Aleksandrov [5, 6]. Based on the Glazer's model, Colla and Reaney have studied the correlation between τ_f and octahedra tilt in the Ba- and Sr-based 1:2 ordered complex perovskite systems [7, 8].

$Ba(Mg_{1/3}Nb_{2/3})O_3$ ceramics, one of the complex perovskites, have high values of ε_r (32), and Q value ($Q * f_o = 56,000$) [9]. These ceramics, however, have relatively high τ_f (33 ppm/°C) compared with those of other complex perovskites [2, 9, 10]. The temperature coefficient of resonant frequency of BMN can be tailored by the addition of the materials with a negative τ_f value. $La(Mg_{2/3}Nb_{1/3})O_3$ has the value $\tau_f = -86$ ppm/°C, $\varepsilon_r = 26.8$ and $Q * f_o = 52,000$ [11]. A solid solution of BMN and LMN therefore is expected to have zero τ_f with high Q-value and ε_r. However, the crystal structures of BLMN and LMN have not been studied. Rhombohedral $R\bar{3}$ or orthorhombic *Pbmn* structure was proposed for LMN [12, 13]. However, according to our analysis, they are not the correct structures for LMN. In this work, $(Ba_{1-x}La_x)[Mg_{(1+x)/3}Nb_{(2-x)/3}]O_3$ ceramics with $0 \leq x \leq 1$ were prepared, and the structural transition of BLMN with La content was studied using HRTEM and XRD.

2. Experimental procedures

Specimens of $(Ba_{1-x}La_x)[Mg_{(1+x)/3}Nb_{(2-x)/3}]O_3$, with $0 \leq x \leq 1$ were synthesized by a conventional solid-state reaction method from $BaCO_3$ (Aldrich, 99%), La_2O_3 (Aldrich, 99%), Nb_2O_5 (tritech, 99.9%), and MgO (Junsei, 99%). The materials were weighed in the appropriate molar ratio and mixed with ZrO_2 balls in an ethanol media for 24 h. The powders were dried, calcined at 1300°C for 4 h in air, and pressed into a disk. These pellets were sintered at 1450°C for 4 h in air. X-ray diffraction pattern (XRD) data for the Rietveld refinement were collected at room temperature with MACScience M18XHF diffractometer. Rietveld refinements were performed using DBWS 9411 [14]. Microstructure of the specimens were studied using high resolution transmission electron

---

[*] Author to whom all correspondence should be addressed.

microscopy (HRTEM). TEM specimens were cut from disc, mechanically ground, and ion milled using argon. Hitachi H-9000NAR TEM were used to examine the specimens.

3. Results and discussion

Fig. 1 shows the X-ray powder diffraction patterns of $(Ba_{1-x}La_x)[Mg_{(1+x)/3}Nb_{(2-x)/3}]O_3$, with $0 \leq x \leq 1$ specimens sintered at 1450°C for 4 h. All the peaks were indexed based on the cubic perovskite unit cell. As seen from the figure, the intensities of the 1:2 ordering superlattice reflections shown in BMN decreased as La content, x, increased, eventually disappearing. When $x > 0.1$, a series of extra peaks at 1/2(111) and 1/2(311) positions — indicated by open circle — began to grow, attaning maxima at $x = 0.5$. When x was above 0.5, the intensity of 1/2(111) extra peak gradually decreased but that of 1/2(311) extra peak has not been changed. The extra peak at 1/2(111) position has formed as a result of the 1:1 chemical ordering of cations. Because two types of ions existed in both the A and B sites, the 1:1 chemical ordering could occur in the A sites and/or B sites. However, since the 1:1 ordering also was found in LMN which had only La ions in the A site, the 1:1 ordering was considered restricted in B sites. The same results were found by other investigators for the systems $(Pb_{1-x}La_x)[Mg_{(1+x)/3}Nb_{(2-x)/3}]O_3$ and $(Ba_{1-x}La_x)[Zn_{(1+x)/3}Ta_{(2-x)/3}]O_3$ [15, 16].

The 1/2(311) extra peak shown in Fig. 1 could arise from the 1:1 chemical ordering and/or the anti-phase tilt of octahedra [3, 4, 17]. When $x < 0.7$, the variation of the intesity of 1/2(311) with x was the same as that of 1/2(111) extra peak thus, the 1/2(311) extra peak was thought to be formed due to the 1:1 ordering. On the contrary, when $x > 0.7$, the degree of the 1:1 ordering identified by the 1/2(111) extra peak decreased but the intensity of 1/2(311) extra peak has not been changed. This result implies that when x exceeded 0.7, the 1/2(311) extra peak was associated with the anti-phase tilting of the octahedra as well as the 1:1 chemical ordering. More discussion on the anti-phase tilting of the octahedra will be given in later.

As seen in Fig. 1, BLMN had a 1:1 ordered cubic structure when $0.1 < x < 0.7$. As x exceeded 0.7, however, new extra peaks appeared at the 1/2(210), 1/2(300) and 1/2(410) positions, indicated by closed circles. The anti-parallel shift of the A-site cations is responsible for the presence of those extra peaks [8]. Therefore, when $x > 0.7$, the 1:1 ordered cubic is not the structure of BLMN.

In order to determine the crystal structure of BLMN with $x > 0.7$, the detailed investigation on the crystal structure of LMN has been conducted. Fig. 2 shows the XRD pattern of $La(Mg_{2/3}Nb_{1/3})O_3$ ceramics sintered at 1450°C for 4 h. As can be seen in this figure, a series of extra peaks appeared at the 1/2(111), 1/2(210), 1/2(300), 1/2(311) and 1/2(410) positions. The appearance of the 1/2(111) extra peak was result of the 1:1 chemical ordering of B site ions. The presence of the 1/2(210), 1/2(300) and 1/2(410) extra peaks indicates that the anti-parallel shift of the A-site cations exists in LMN. The 1/2(311) extra peak could arise from the 1:1 chemical ordering and/or the anti-phase tilt of octahedra. In general, the anti-phase tilting of the octahedra precedes the anti-parallel shift of the A-site cations [7]. Therefore, it is thought that the anti-phase tilting of the octahedra exists in LMN and both the 1:1 chemical ordering and the anti-phase tilting were responsible for the formation of the 1/2(311) extra peak.

In order to prove the presence of anti-phase tilting of the octahedra in LMN, the solid solution of $(1-x)La(Mg_{2/3}Nb_{1/3})O_3 - xSrTiO_3$ was formed. Since the $SrTiO_3$ has the cubic structure and only one ion, Ti^{4+}, exists in B site, the lattice distortion and the 1:1 chemical ordering existed in LMN were expected to decrease with the increase of x. Fig. 3 shows the XRD patterns of $(1-x)La(Mg_{2/3}Nb_{1/3})O_3$-$xSrTiO_3$ system sintered at 1500°C for 4 h. As can be seen in this figure, the 1:1 ordering identified by the 1/2(111) extra peak decreased with increasing x and finally disappeared when $x > 0.3$. However, the 1/2(311) extra

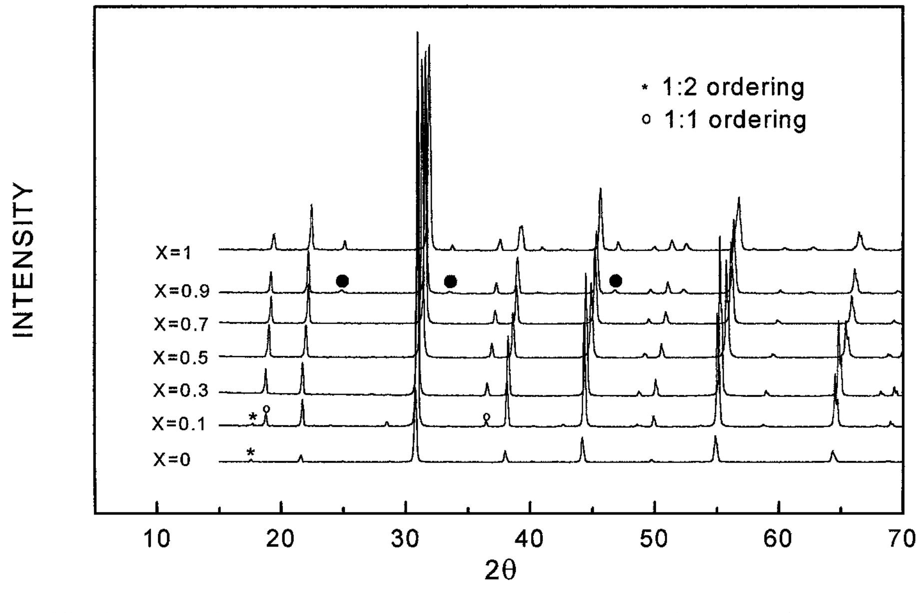

Figure 1 X-ray powder diffraction pattern of $(Ba_{1-x}La_x)(Mg_{(1+x)/3}Nb_{(2-x)/3})O_3$ with $0 \leq x \leq 1$ sintered at 1450°C for 4 h.

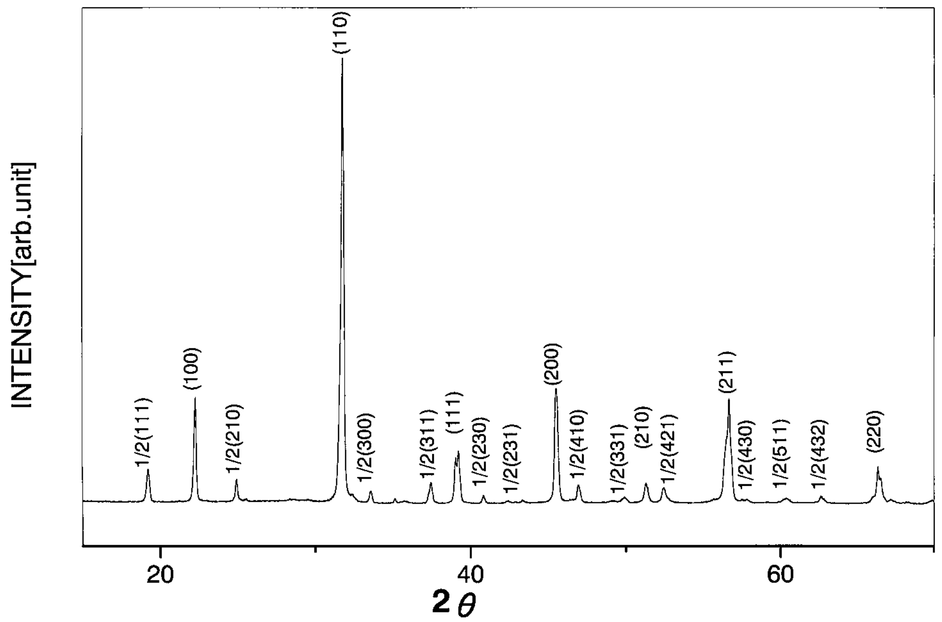

Figure 2 X-ray diffraction pattern of the $La(Mg_{2/3}Nb_{1/3})O_3$ ceramics sintered at 1450°C for 4 h.

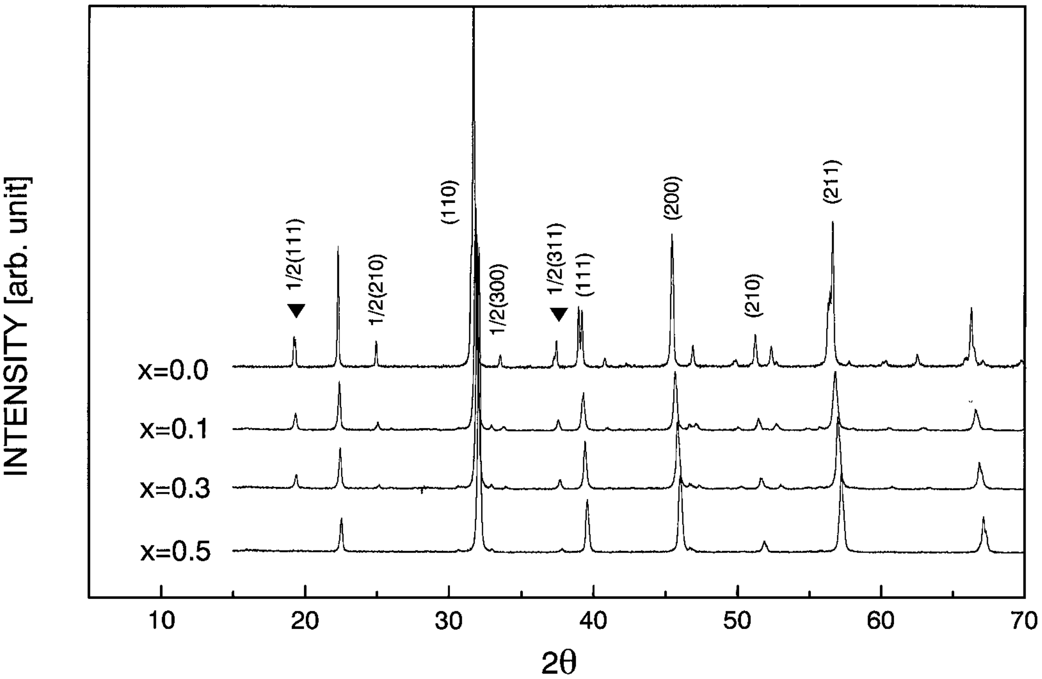

Figure 3 X-ray diffraction pattern of $(1-x)La(Mg_{2/3}Nb_{1/3})O_3 - xSrTiO_3$ ceramics sintered at 1500°C for 4 h.

peak existed up to $x = 0.5$. Since the 1:1 ordering disappeared as x exceeded 0.3, the existence of 1/2(311) extra peak in the specimen with $x > 0.3$ is explained by the anti-phase tilting of octahedra. This result implies that the 1/2(311) extra peak in LMN is associated with both the 1:1 ordering and the anti-phase tilting of the octahedra. The extra peaks for the in-phase tilting of the octahedra were not found in XRD pattern. However, since the in-phase tilting and the anti-parallel shift of A-site cations occurred simultaneously [7], the in-phase tilting was believed to exist in LMN and TEM results which will be shown in later showed the presence of in-phase tilting.

Rietveld refinement was carried out to determine the crystal structure of LMN. The refined results are summarized in Table I. First, the rhombohedral $R\bar{3}$ model suggested by Lin *et al.* was tested [12]. As shown in Table I. R-factors produced by this model were high. Moreover, in rhombohedral $R\bar{3}$ structure, the in-phase tilting of octahedra which exists in LMN is not allowed [3, 4]. Therefore, LMN can't have the rhombohedral $R\bar{3}$ structure. The orthorhombic structure Pbmn was also tested. R-factors of this structure were low as listed in Table I. However, the 1:1 chemical ordering is not

TABLE I Summary of Rietveld refinement for $La(Mg_{2/3}Nb_{1/3})O_3$ ceramics

Space group	R_p	R_{wp}	R_e	χ
$R\bar{3}$	14.09	17.87	4.41	4.06
Pbnm	9.07	12.69	4.39	2.89
$P2_1/n$	7.34	10.06	4.40	2.28

χ : Goodness of fit.
$\chi^2 = (R_{wp}/R_{exp})^2$

TABLE II Refined lattice parameters, fractional atomic coordinates, thermal parameters and occupancies of La($Mg_{2/3}Nb_{1/3}$)O_3 ceramics

Lattice parameter
$a = 5.6004(4)$ Å $b = 5.6414(4)$ Å $c = 7.9346(5)$ Å $\beta = 89.9819(3)°$

Atoms	Positional and thermal displace parameters from X-ray refinement x	y	z	B	Occup.
La	0.5046(3)	0.5331(1)	0.2511(2)	2.1841(6)	1.00000
Mg(B′)	0.00000	0.50000	0.00000	1.1015(2)	0.50000
Mg(B″)	0.50000	0.00000	0.00000	1.4384(4)	0.0983(4)
Nb(B″)	0.50000	0.00000	0.00000	1.4384(4)	0.4017(4)
O_1	0.2901(6)	0.2725(6)	0.0326(2)	0.9239(9)	1.00000
O_2	0.2427(4)	0.7814(3)	0.0707(1)	0.9239(9)	1.00000
O_3	0.4362(8)	0.9821(6)	0.2543(5)	0.9239(9)	1.00000

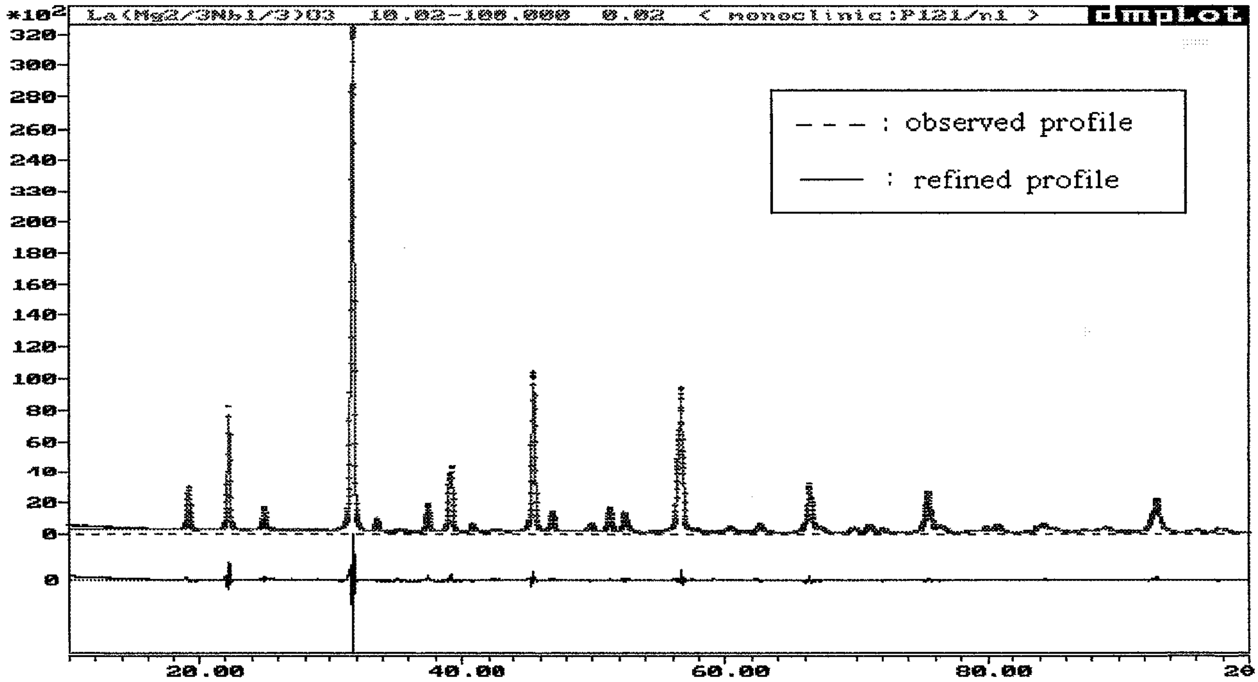

Figure 4 Observed and refined X-ray diffraction pattern of La($Mg_{2/3}Nb_{1/3}$)O_3.

allowed in this structure. Therefore, the extra peak at 1/2(111) position (odd-odd-odd reflection) should be explained by the anti-phase tilting of octahedra [3, 4]. However, according to the work of Glazer, the lowest-order reflection due to the anti-phase tilting is 1/2(311) [3, 4]. Moreover, the behavior of the extra peak at 1/2(111) position shown in Fig. 2 is different from that of 1/2(311) peak. Therefore, the extra peak at 1/2(111) position can't be explained by the anti-phase tilting of octahedra and only the 1:1 chemical ordering can explain the existence of the 1/2(111) extra peak. As a result, the orthorhombic Pbmn is not the structure of LMN.

Finally, monoclinic structure $P2_1/n$ which has both the 1:1 chemical ordering and $a^- \ a^- \ c^+$ (or $a^- \ a^- \ a^+$) tilting axis was tested [18]. As shown in Table I, $P2_1/n$ model produced the most successful refinement results. The observed and calculated X-ray diffraction pattern is shown in Fig. 4. Refined atomic parameters and interatomic distances are given in Tables II and III, respectively. The refined lattice parameters are $a = 5.6004$ Å, $b = 5.6414$ Å, $c = 7.9346$ Å, and $\beta = 89.9819°$. The pseudocubic unit cell lengths of LMN which were used by Glazer to denote the tilting system are $a_p = b_p = 0.3927$ nm and $c_p = 0.3921$ nm [3, 4]. Therefore, LMN has $a^- \ a^- \ c^+$ tilting system. The X-ray diffraction pattern of LMN is the same as those of BLMN with $x > 0.7$. Thus, it can be concluded that BLMN specimens with $x > 0.7$ also have the 1:1 ordered monoclinic structure.

TABLE III Selected atomic distances (Å) of La($Mg_{2/3}Nb_{1/3}$)O_3 ceramics

MgO$_6$-octahedron			LaO$_8$-polyhedron		
Mg-O_1	2.0868	2×	La-O_1	2.5711	1×
Mg-O_2	2.1639	2×		2.7372	1×
Mg-O_3	1.9849	2×		2.7547	1×
Mean	2.0785		La-O_2	2.4359	1×
Shannon	2.1			2.4824	1×
				3.0508	1×
NbO$_6$-octahedron			La-O_3	2.4853	1×
Nb-O_1	1.9522	2×		2.5620	1×
Nb-O_2	1.9777	2×	Mean	2.6350	
Nb-O_3	2.0514	2×	Shannon	2.54	
Mean	1.9938				
Shannon	2.02				

Transmission electron microscopy studies were performed to investigate in detail variations in the crystal structure of BLMN with La content. Fig. 5a to d represent the HRTEM images and electron diffraction patterns of BLMN with $x = 0$, 0.1, 0.5 and 0.9, respectively. As seen Fig. 5a, the 1:2 ordered hexagonal structure was well developed in BMN, and that structure was found in the entire area of BMN. In the case of BLMN with $x = 0.1$, both the 1:2 and 1:1 ordered structures coexisted, as shown in Fig. 5b. Most of the area, however, has the 1:1 ordered cubic structure. The results shown in Fig. 5a and b indicate that a small amount of La substitution destroyed the 1:2 ordered hexagonal structure and caused a 1:1 ordered cubic structure. Fig. 5c shows the HRTEM image and diffraction pattern of the specimen with $x = 0.5$. Only the 1:1 ordered cubic structure was found in that specimen. Similar results were obtained for the specimens with $0.1 < x \leq 0.7$.

Fig. 5d shows the HRTEM image of the [100] zone axis obtained from the BLMN with $x = 0.9$. The inset represents the [100] electron diffraction pattern taken from the same area. The extra reflections at 1/2{210} and 1/2{300} which are due to the anti-parallel shift of

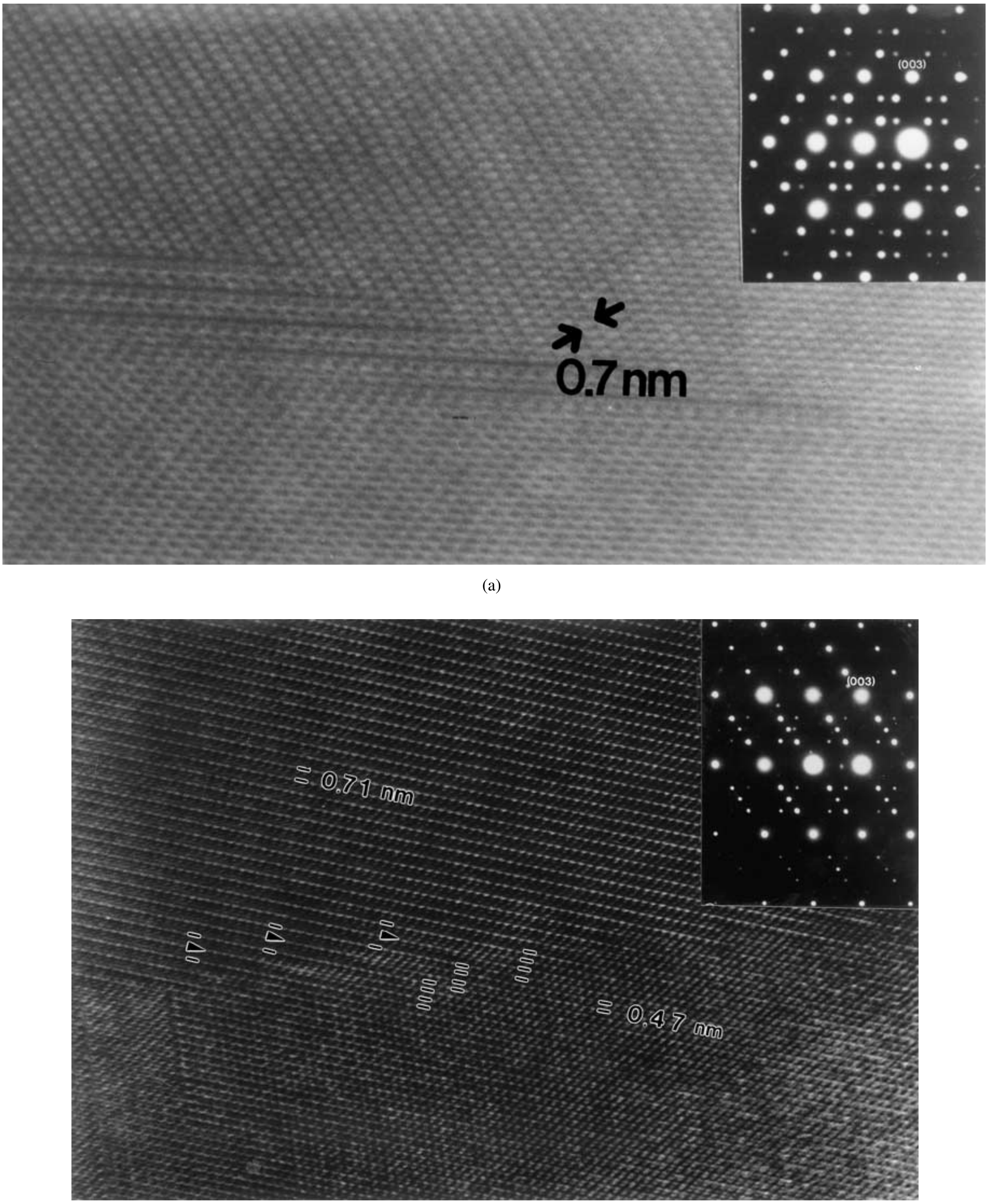

(a)

(b)

Figure 5 HRTEM images and electron diffraction patterns of (a) $Ba(Mg_{1/3}Nb_{2/3})O_3$, (b) $(Ba_{0.9}La_{0.1})(Mg_{1.1/3}Nb_{1.9/3})O_3$, (c) $(Ba_{0.5}La_{0.5})(Mg_{1/2}Nb_{1/2})O_3$ and (d) $(Ba_{0.1}La_{0.9})(Mg_{1.9/3}Nb_{1.1/3})O_3$. (*Continued.*)

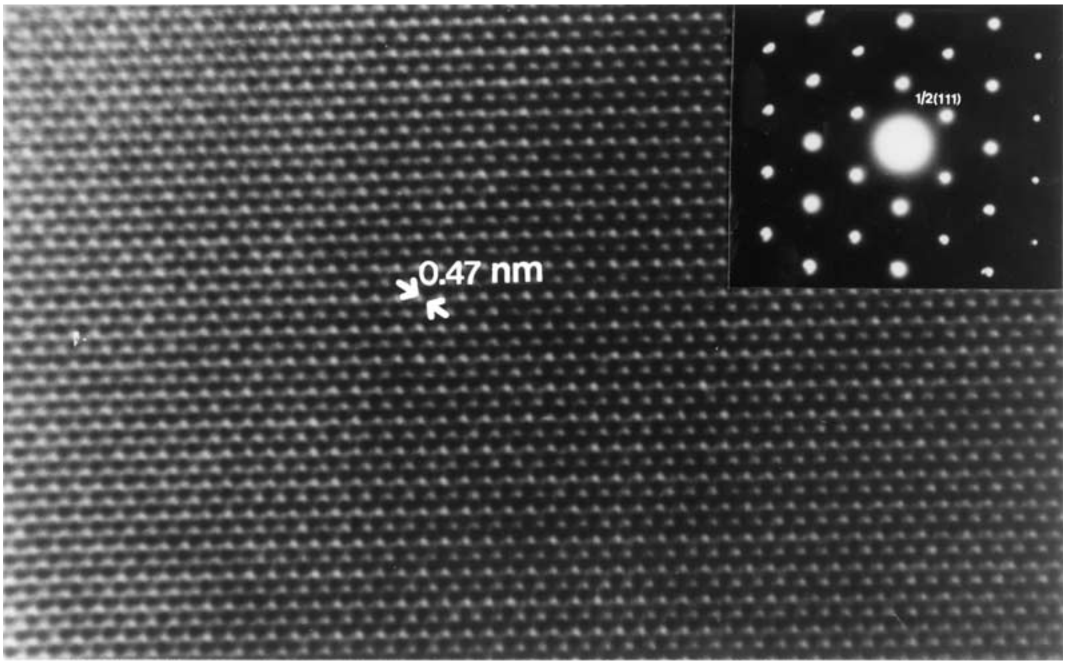

(c)

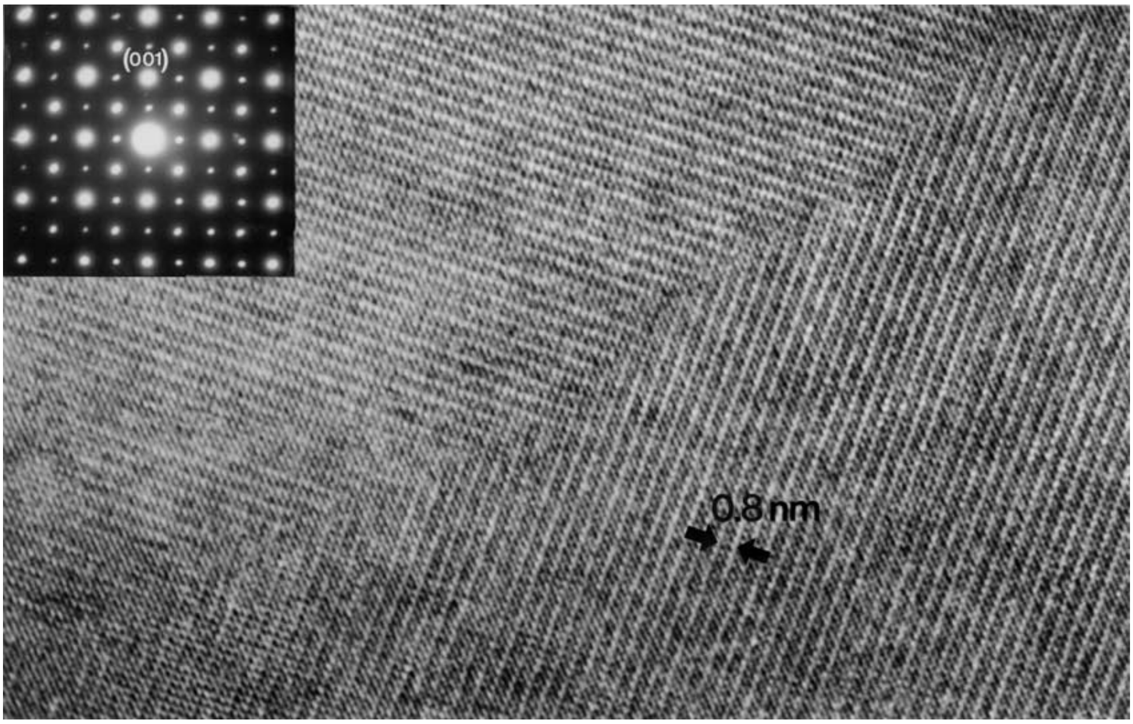

(d)

Figure 5 (*Continued*).

the A-site cations were observed in this pattern. Moreover, the 1/2{100} 1/2{100} superlattice reflections that were not observed in XRD pattern were obtained in electron diffraction pattern. The HRTEM image also shows the new type of modulation along the [010] and [001] directions with the wavelength of 0.8 nm. According to the previous work, the 1/2{100} and 1/2{110} superlattice reflections were associated with the anti-parallel shift of the A-site cations and the in-phase tilting of the oxygen octahedra, respectively. Therefore, TEM analysis clearly showed the presence of the in phase tilting of oxygen octahedra in BLMN with $x > 0.7$.

Fig. 6a shows the HRTEM image with [001] zone axis taken from LMN specimen. The inset represents the electron diffraction pattern taken from the same area. The diffraction pattern shows the 1/2{110} superlattice reflections indicating the presence of the in phase tilting of oxygen octahedra in LMN. Those superlattice reflections give rise to modulation along the [110] directions, with a wavelength of 0.56 nm in the HRTEM image shown in Fig. 6a. Fig. 6b shows the [100] zone axis HRTEM image and electron diffraction pattern. The diffraction pattern exhibits 1/2{100} superlattice reflections in two directions. Those 1/2{100} superlattice reflections give rise to two independent set of

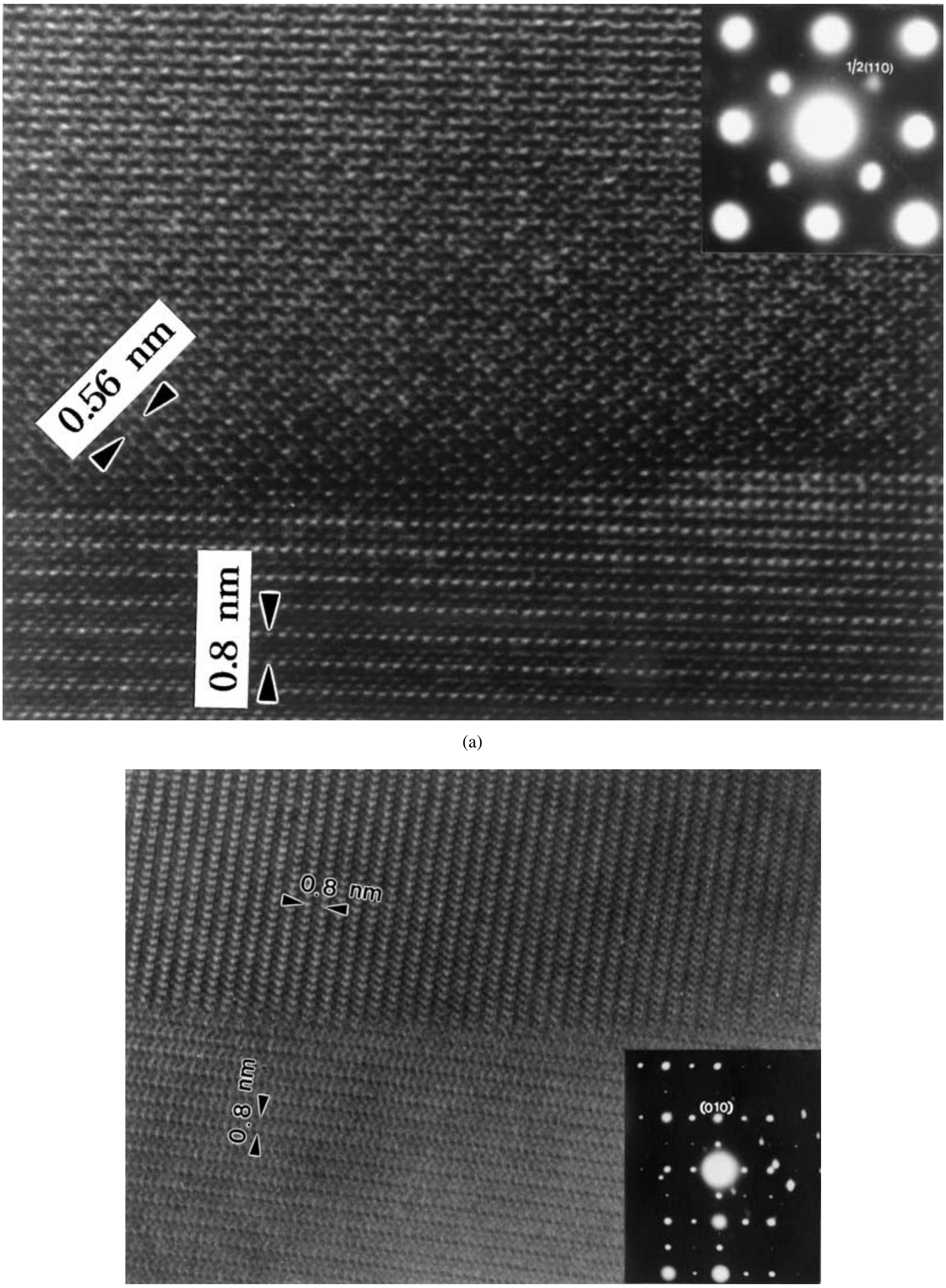

(a)

(b)

Figure 6 HRTEM image and electron diffraction pattern of LMN with (a) [001] zone axis and (b) [100] zone axis.

1/2{100} lattice fringe, seen in HRTEM image. The 1/2{100} superlattice reflections in different directions therefore arose from the different varients.

4. Conclusions

Variation in the crystal structure of $(Ba_{1-x}La_x)(Mg_{(1+x)/3}Nb_{(2-x)/3})O_3$ with $0 \leq x \leq 1$ was investigated in the present study. A 1:2 ordered hexagonal structure was found in the whole region of BMN. With increased La content, the structure changes to the 1:1 ordered cubic. When $x = 0.1$, both 1:1 and 1:2 ordered structures were found but most of the area had the 1:1 ordered cubic structure. The 1:1 ordered cubic structure was maintained up to $x = 0.7$. When x exceeded 0.7, however, BLMN is transformed from a 1:1 ordered cubic to a 1:1 ordered monoclinic structure. The 1:1 ordered monoclinic BLMN had both the in–phase and anti–phase tilting of oxygen octahedra. $La(Mg_{2/3}Nb_{1/3})O_3$ has the 1:1 ordered monoclinic $P2_1/n$ structure. The lattice parameters of $La(Mg_{2/3}Nb_{1/3})O_3$ are $a = 5.6004$ Å, $b = 5.6414$ Å, $c = 7.9346$ Å, and $\beta = 89.9819°$. The 1:1 ordered monoclinic $La(Mg_{2/3}Nb_{1/3})O_3$ is distorted by the in-phase and the anti-phase tilting of octahedra with the $a^- a^- c^+$ tilting system. The anti-parallel shift of A-site cations was also found in $La(Mg_{2/3}Nb_{1/3})O_3$.

Acknowledgments

This work was supported by the Ministry of Information and Communication.

References

1. W. WERSING, "Electronic Ceramics," edited by B. C. H. Steele (Elsevier Science, New York, 1991) ch. 4, p. 69.
2. S. B. DESU and H. M. O'BRYAN, *J. Amer. Ceram. Soc.* **68**(10) (1985) 546.
3. A. M. GLAZER, *Acta Cryst.* B **28** (1972) 3384.
4. *Idem.*, *ibid.* A **31** (1975) 756.
5. K. S. ALEKSANDROV, *Ferroelectronics* **14** (1976) 801.
6. *Idem.*, *ibid.* **20** (1978) 61.
7. E. L. COLLA, I. M. REANEY and N. SETTER, *J. Appl. Phys.* **74** (1993) 3414.
8. I. M. REANEY, E. L. COLLA and N. SETTER, *Jpn. J. Appl. Phys.* **33** (1994) 3984.
9. S. NOMURA, *Ferroelectronics* **49** (1983) 61.
10. H. MASUMOTO, H. TAMURA and K. WAKINO, *Jpn. J. Appl. Phys.* **30**(9B) (1991) 2347.
11. J. H. PAIK, C. H. CHOI, S. NAHM, J. D. BYUN and H. J. LEE, *J. Mater. Sci. Lett.* **18** (1999) 889.
12. L. J. LIN and T. B. WU, *J. Amer. Ceram. Soc.* **74**(6) (1991) 1360.
13. J. S. KIM, C. I. CHEON, H. J. KANG, H. S. SHIM, C. H. LEE, S. NAHM and J. D. BYUN, *Mater. Lett.* **38** (1999) 294.
14. R. A. YOUNG, A. SAKTHIVEL, T. S. MOSS and C. O. PAIVA-SANTOS, "User's Guide to Program DBWS-9411" (School of Physics, Georgia Institute of Techonology, 1995).
15. L. J. LIN and T. B. WU, *J. Amer. Ceram. Soc.* **73**(5) (1990) 1253.
16. C. C. LEE, C. C. CHOU and D. S. TSAI, *ibid.* **80**(11) (1997) 2885.
17. H. J. YOUN, K. S. HONG and H. KIM, *J. Mater. Res.* **12**(3) (1996) 589.
18. P. M. WOODWARD, *Acta Cryst.* B **53** (1997) 44.

Received 7 July 1999
and accepted 24 September 2002